J Therm Anal Calorim (2018) 131:925–935
https://doi.org/10.1007/s10973-017-6595-7

A facile synthesis of boron nanostructures and investigation of their catalytic activity for thermal decomposition of ammonium perchlorate particles

Seyed Ghorban Hosseini[1] · Mohammad Ali Zarei[1] · Seyed Jafar Hosseini Toloti[2] · Hamid Kardan[1] · Mohammad Amin Alavi[3]

Received: 11 March 2017 / Accepted: 15 July 2017 / Published online: 27 July 2017

Abstract In this research, ultrasound irradiation as a simple method was used to produce boron nanostructures. Reaction conditions such as boron concentration and sonication time show important roles in the size, morphology and growth process of the final products. The boron nanostructures (nanoparticles and nanorods) were characterized by scanning electron microscopy, transmission electron microscopy, X-ray powder diffraction, small-angle X-ray scattering and inductively coupled plasma atomic emission spectroscopy techniques. Primary evaluation of results showed that nanoparticles and nanorods of boron successfully have been prepared with 25–40 and 50–100 nm average particle size, respectively. These nanostructures (nanoparticles and nanorods) were studied as an additive for promoting the thermal decomposition of ammonium perchlorate (AP) particles. Thermochemical decomposition behaviors of treated samples were characterized by thermal gravimetric analysis and differential scanning calorimetry techniques. Also, the kinetic parameters of thermal decomposition processes of pure and treated samples were obtained by nonisothermal methods proposed by Kissinger and Ozawa. However, boron nanoparticles with the smallest average particle size (25–40 nm) have the most significant catalytic effect including the decrease in decomposition temperature of AP + B nanocomposite by 100 °C, increase in the heat of decomposition from 580 to 1354 J g^{-1} and decrease in activation energy from 207 to 110 kJ mol^{-1}.

Keywords Boron nanostructures · Ultrasound irradiation · Ammonium perchlorate (AP) · Catalytic activity · Kinetic parameters

Introduction

Elemental boron is appealing for use as an enhancing agent in combustion applications due to its high theoretical energy density, both on a volumetric and a gravimetric bases [1]. This coupled with a high energy of combustion, a high combustion temperature and low molecular weight products, explains why boron is considered an attractive material for use in rocket propellants and explosives mixtures [2].

Boron is a typical energetic material which produces high heat by oxidation reaction. Thus, fine boron particles are expected to be used as fuels for solid-fueled ramjets [3]. Indeed, there are a number of previous reports on production of boron at nanosizes using methods such as gas-phase pyrolysis of diborane or solution-based synthesis routes [4–6].

Sonochemistry is the research area in which molecules undergo a chemical reaction due to the application of powerful ultrasound radiation (20 kHz–10 MHz) [7]. In the recent years, many kinds of nanomaterials have been prepared by this method [8–12]. In the present work, we have developed a simple sonochemical method to prepare nanostructures of boron.

✉ Seyed Ghorban Hosseini
hoseinitol@yahoo.com

[1] Department of Chemistry, Malek Ashtar University of Technology, P.O. Box: 16765-3454, Tehran, Islamic Republic of Iran

[2] Babol Education Department, Babol, Islamic Republic of Iran

[3] Department of Chemistry, Faculty of Sciences, Tarbiat Modares University, P.O. Box 14117-13116, Tehran, Islamic Republic of Iran

Ammonium perchlorate (AP) is the most common energetic material that is widely used as an oxidizer in composite solid propellants, fireworks, pyrotechnics, explosives, an ingredient of matches, a component of air bag inflators and in analytical chemistry [13, 14]. AP is also known as a special and hardly replaceable oxidizer agent in the rocket fuel due to its high oxygen content (54.5% w w^{-1}) and to the fact that it leaves no solid residue upon its thermal decomposition. The fraction of AP in the composite solid rocket fuels is usually up to 70% by mass [15]. However, considering the limited loading of AP or their composites in the rocket, it is crucial to further improve its decomposition efficiency to produce large amount of energy as far as possible and to decrease its burning temperature for easy operation and control. In contrast to the nanoparticles of metal oxide, the pure metal nanoparticles are much sensitive to the oxygen and may be effective to improve the decomposition efficiency of AP. Such proposition is supported by the effect of Ni nanoparticles in increasing their burning efficiency and burning velocity for other propellants [16]. Many investigations have been carried out on the catalytic activity of metal oxides on thermal decomposition of AP particle [16–23], but these with pure metal or nonmetal compound have rarely been performed [16, 17]. Furthermore, to the best of our knowledge there is no report on the catalytic activity of nanorods and nanoparticles of boron on thermal decomposition of ammonium perchlorate particles.

The present work is aimed to prepare nanostructures of boron by ultrasound irradiation and to study the effects of some synthesis parameters such as concentration of boron and sonication time which affect the distribution and growth of boron nanostructures. The boron nanostructures (nanoparticles and nanorods) were characterized by scanning electron microscopy (SEM), transmission electron microscopy (TEM), X-ray powder diffraction (XRD), small-angle X-ray scattering (SAXS) and inductively coupled plasma atomic emission spectroscopy (ICP-AES) techniques. Finally, the catalytic activities of boron nanostructures (nanoparticles and nanorods) at optimum synthesis condition have been investigated on the thermal decomposition of ammonium perchlorate (AP) particles by thermal analysis methods. Also, in order for the better evaluation of results, the effect of microboron particles on thermal decomposition of AP was investigated. However, similar experimental analysis was done with microboron particles and the results were compared with nanocatalytic results. Solvent–nonsolvent method, as a conventional microencapsulation technique, has been examined to obtain proper AP + B nanocomposites samples. Differential scanning calorimetry (DSC) and thermogravimetry (TG) analysis methods were used to investigate the thermal decomposition behavior of AP in the presence of boron nanostructures (nanoparticles and nanorods) with diverse average particle size (APS). Finally, based on the thermal analysis data, kinetic parameters for thermal decomposition processes of pure and AP + B nanocomposites have been estimated by nonisothermal methods that were proposed by Kissinger and Ozawa.

Experimental

Materials

All chemical reagents were of analytical grade and used as received without further purification. Ammonium perchlorate (NH_4ClO_4) powder with mean particle size of 80–100 μm as the target and ethanol and methyl isobutyl ketone (99% purity) were all purchased from Merck (Tehran, Iran). Amorphous boron precursor with mean particle size of 1 μm as raw materials was prepared by magnesiothermic reduction [18]. Water used in these experiments was deionized and doubly distilled.

Preparation of boron nanostructure

Bulk amorphous boron was prepared by magnesiothermic method as described in literatures [18]. So, as-prepared bulk boron was used as a precursor to produce nanoboron powder by sonochemical method. Ultrasonic generator was carried out on an ultrasonic bath SONICA 2200 EP (frequency of 40 kHz). In a representative experiment (sample B1, Table 1), 70 mg of the boron precursor with mean particle size of 1 μm was dispersed in 30 mL ethanol and influenced by ultrasound irradiation (frequency of 40 kHz and sonication time 90 min). Then, the prepared sample was filtered and washed with methyl isobutyl ketone (99% purity) as inert solvent three times and dried at ambient temperature. In order to find out the role of different factors

Table 1 Experimental condition, morphology and mean size of synthesized boron nanostructures

Sample no.	Boron/mg	Sonication time/min	Morphology	Mean size/nm
B1	70	90	Particle	50–70
B2	70	60	Rod	50–100
B3	70	30	Particle	60–100
B4	35	30	Particle and rod	25–90
B5	35	60	Particle	80–350
B6	35	90	Particle	25–40
B7	140	90	Particle	200–500
B8	210	90	Particle	250–700

In all experiments, 30 mL ethanol was used as medium in order for the dispersion of bulk boron

such as the aging time of the reaction in the ultrasonic device and the concentration of the boron precursor on the morphology of the nanostructures, these reactions have performed in several conditions (Table 1).

Preparation of AP + B nanocomposite

AP + B nanocomposites (2 or 5% mass of nanoparticles and nanorods boron) were prepared using the solvent–nonsolvent procedure as a fast, scalable and low-cost preparation method [24]. In this study, water and MIBK were chosen as the solvent and nonsolvent, respectively. In representative experiments (sample AP7, Table 2), first, 0.05 g of the freshly prepared boron nanoparticles, B6 (5% by mass with respect to total amount of NH_4ClO_4), was dispersed uniformly in 25 mL MIBK by the ultrasonic apparatus for 15 min. Also, 0.95 g AP was dissolved into 10 mL of water to make a saturated solution at 80 °C. The saturated solution of AP was added dropwise into the boron NPs solution to obtain a nanocomposite of AP + B6. Then, the reaction lasted for several minutes until all the AP was deposited on the surface of the boron nanoparticles. Based on Table 2, the same trend was used in order to prepare AP + Bμ composite (samples AP2-3). Finally, the coated particles (i.e., composites) were filtered, washed with 25 mL MIBK as a nonsolvent three times and dried at ambient temperature.

Characterization of boron nanostructure

Structure, purity, morphology and size of the synthesized boron nanostructures were determined by several techniques. All prepared samples were characterized with a scanning electron microscope (SEM) (Philips XL 30) and (LEO 1450vp) with gold coating and also a transmission electron microscope (TEM) (EM 900 of Zeiss Company) at an accelerating voltage of 80 kV. X-ray powder diffraction (XRD) measurements were performed using an X'pert diffractometer of Philips Company with monochromated Cukα radiation ($\lambda = 0.15405$ nm), and small-angle X-ray scattering (SAXS) measurement were performed by X'pert Pro MPD of PANalytical Company by easy SAXS software analyzer. Inductively coupled plasma atomic emission spectroscopy (ICP-AES) was performed using Perkin Elmer 53,000 V.

Table 2 Results of the thermal decomposition of AP in the presence of 2 and 5% of different boron micro- and nanoparticles (μ, B2 and B6) ($\beta = 10$ C min^{-1})

Sample no./component	Percent/%	Peak T_m/°C		Δm		ΔH/J g^{-1}
		LTD/°C	HTD/°C	Δm_1/%	Δm_2/%	
AP1/(Pure AP)	100	305.5	402.6	29	70	580
AP2/(AP + Bμ)	98/2	310.0	405.2	25	75	495.0
AP3/(AP + Bμ)	95/5	314.0	412.3	30	70	458.0
AP4/(AP + B2)	98/2	–	356.8	–	98	995
AP5/(AP + B2)	95/5	–	331.0	–	100.0	1053
AP6/(AP + B6)	98/2	–	312.8	–	97.9	1287
AP7/(AP + B6)	95/5	–	301.5	–	100.0	1354

Thermal characterization of AP + B nanocomposite

The catalytic effects of boron micro, nanoparticles and nanorods on the thermal decomposition properties of NH_4ClO_4 particles were characterized by differential scanning calorimetry (DSC) and thermogravimetry analysis (TG) techniques. The DSC curves were obtained by Shimadzu differential scanning calorimetry, model DSC-60, in a temperature range of 25–600 °C using an aluminum crucible with a single hole punched in the lid at the heating rates (β) of 5, 10, 15, 20 °C min^{-1} under argon atmosphere. The instrument was calibrated using a dedicated 1-mg indium standard in an aluminum pan. Plotting for exothermic reactions was a downward deflection of the curve peak from the baseline. Thermogravimetry analysis (TG) was carried out using a Stanton Redcroft, STA-780 series with an alumina crucible, applying a heating rate of 10 °C min^{-1} in a temperature range of 25–600 °C under argon atmosphere with the flow rate of 50 mL min^{-1}. The average sample mass was about 2–5 mg.

Results and discussion

SEM analysis

Figure 1 shows SEM images of boron nanostructures prepared by influencing ultrasound irradiation to amorphous microsize bulk boron. Experimental condition and morphology and mean size of obtained boron nanostructures are summarized in Table 1. Primary evaluation of the summarized results in Table 1 and Fig. 1 confirmed that some synthesis parameters such as concentration of bulk boron and sonication time affect the distribution and growth of boron nanostructures.

Effect of synthesis parameters

The effects of some synthesis parameters such as sonication time and boron precursor concentration on the size and morphology of obtained nanostructures were investigated.

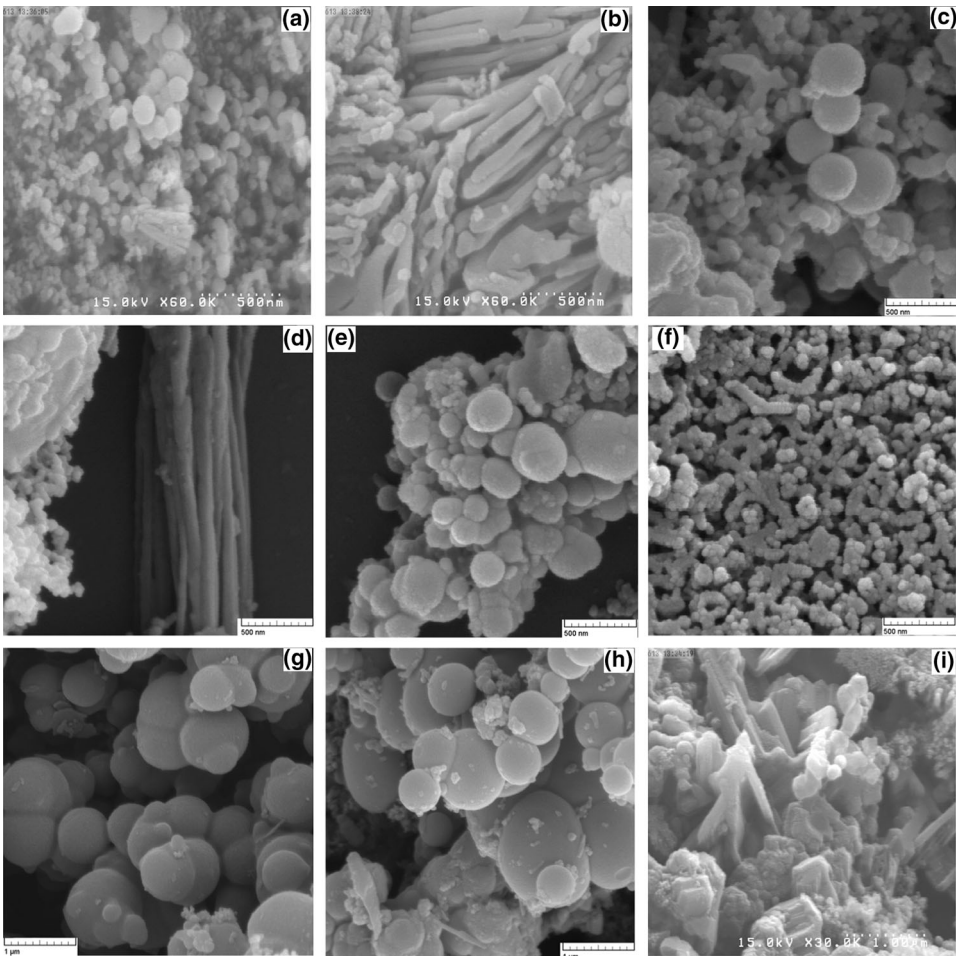

Fig. 1 SEM images of boron nanostructures prepared by influencing ultrasound irradiation to bulk boron B1–8 (**a**–**h**) and **i** as-prepared boron precursor

Sonication time

Seventy micrograms of boron was dispersed in 30 mL ethanol, and the effect of ultrasound irradiation in three different times 30, 60 and 90 min has been investigated. As it can be seen in Fig. 1a–c, in 70 mg of boron, ultrasound irradiation in 60 min leads to one-dimensional nanostructures of boron as B2 (Fig. 1b). By further sonication (sample B1), there are lots of nanoparticles that are uniform but still some nanorods remain. It seems by increasing sonication time from 60 to 90 min, ultrasound irradiation physically breaks one-dimensional boron to nanoparticles (Fig. 1a). By reducing sonication time till 30 min (sample B3), there are only nano- and microparticles of boron, and it means that ultrasound irradiation needs more than 30 min to affect physically the microboron and break and grow them at nanosizes.

Boron concentration

To know the effect of boron concentration and sonication time together, 35 mg of boron precursor influenced by ultrasound irradiation at 30, 60 and 90 min, as it can be seen in Fig. 1d–f, by reducing concentration of boron compared to sample B3 in 30 min, one-dimensional nanorods of boron grew (sample B4). It means that for lower concentration of boron lower sonication time is need to grow one-dimensional nanostructures (Fig. 1d). By increasing sonication time to 60 min, one-dimensional nanostructures break and nano- or microparticles of boron have been prepared (Fig. 1e, sample B5). As it can be seen in Fig. 1f, further increase in sonication time till 90 min leads to uniform and well-distributed particles of boron (sample B6).

To know the effect of precursor concentration, two further amount of boron 140 and 210 mg have been dispersed in ethanol and affected by ultrasound irradiation for 90 min. Microparticles of boron have been prepared, but for both samples B7 and B8 (Fig. 1g, h) particles are uniform but bigger than sample B6. It seems that at lower concentration of precursor ultrasound irradiation could break the particles to the seeds; then, at period of sonication the seeds could join together at one direction to prepare one-dimensional nanostructures.

Figure 1i shows SEM images of as-prepared microboron by magnesiothermic reduction (bulk sample). As it can be seen, the size and morphology of bulk boron particles are not uniform. The results confirm that by influencing ultrasound irradiation on the bulk sample, size and morphology of particles have been changed. So ultrasound irradiation has physical effect on bulk boron to produce nanostructures. The effects of some synthesis parameters such as sonication time and boron precursor concentration on the size and morphology of nanostructures are summarized in Table 1.

Particle size histogram of samples B1, B3 and B6 is illustrated in Fig. 2. The presented results show that the most of the particles sizes are in the range from 50 to 70 nm for sample B1. By decreasing the sonication time to 30 min, as particle size histogram shows in Fig. 2b, most of particles sizes are in the range of 60–100 nm. Also based on Fig. 2c, most of particles in sample B6 are in the range of 25–40 nm, which is the best distribution in all samples.

Characterization of structure, morphology and size of boron nanostructures

The morphology, structure and size of the sample B6 were investigated, and the results illustrated in Fig. 3. XRD pattern of as-prepared nanoboron by sonochemistry method (sample B6) is shown in Fig. 3a. As it has been seen, ultrasound irradiation does not effect crystallinity, and in this study, XRD pattern of prepared nanostructures is not in agreement properly with JCPDS cards number 00-023-0063 and has more amorphous than crystalline structure. The XRD result showed micronized amorphous raw materials resulting in nanosized amorphous ones in ultrasound irradiation method.

High temperature and pressure take place in sonochemical method (cavitation), resulting in some components that adsorbed on surface of microparticles were solved in reaction media and improved the purity of product. As-prepared boron by magnesiothermic method and sample B6 was characterize by ICP-AES to clarify boron purity. The result shows that boron precursor has 83% purity and nanostructures of boron have 85% purity.

TEM analysis for sample B6 is illustrated in Fig. 3b, c. The result is in agreement with SEM images. As it can be seen, most of the particles are around 30 nm and some of the particles are going to growth in one dimension. To confirm TEM analysis results, small-angle X-ray scattering (SAXS) analysis were performed on sample B6. As it can be seen in Fig. 3d, average radius for particles is 31 nm that is in agreement with TEM and SEM analyses results.

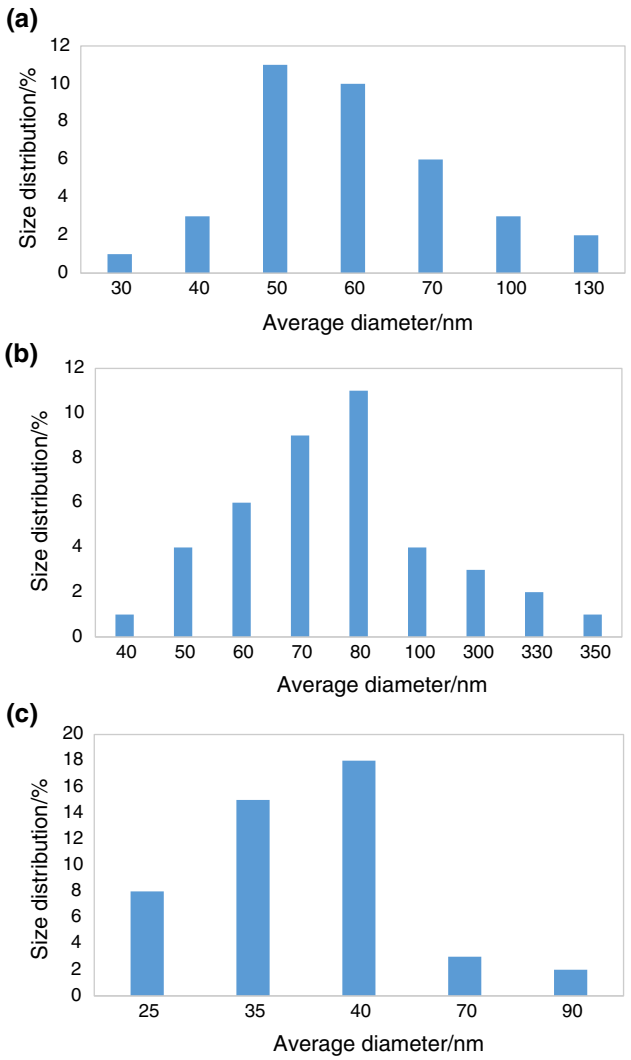

Fig. 2 Particle size histogram of synthesized boron nanoparticles samples, B1 (**a**), B3 (**b**) and B6 (**c**)

Thermal properties of samples

Thermal analysis for pure AP, AP + Bμ, AP + B2 (nanorods) and AP + B6 (nanoparticles) has been investigated, and the results illustrated in Fig. 4a–d, respectively.

Thermal analysis of pure AP particles

In alignment with literature results and as shown in Fig. 4a, the thermal decomposition of pure AP occurs through three consecutive processes. First, an endothermic process takes place at 244.8 °C which is assigned to a solid-state phase transition from the orthorhombic to the cubic phase. Subsequent event occurs exothermically at the temperatures lower than 350 °C, namely low-temperature decomposition (LTD = 305.5 °C), and ascribed to the partial

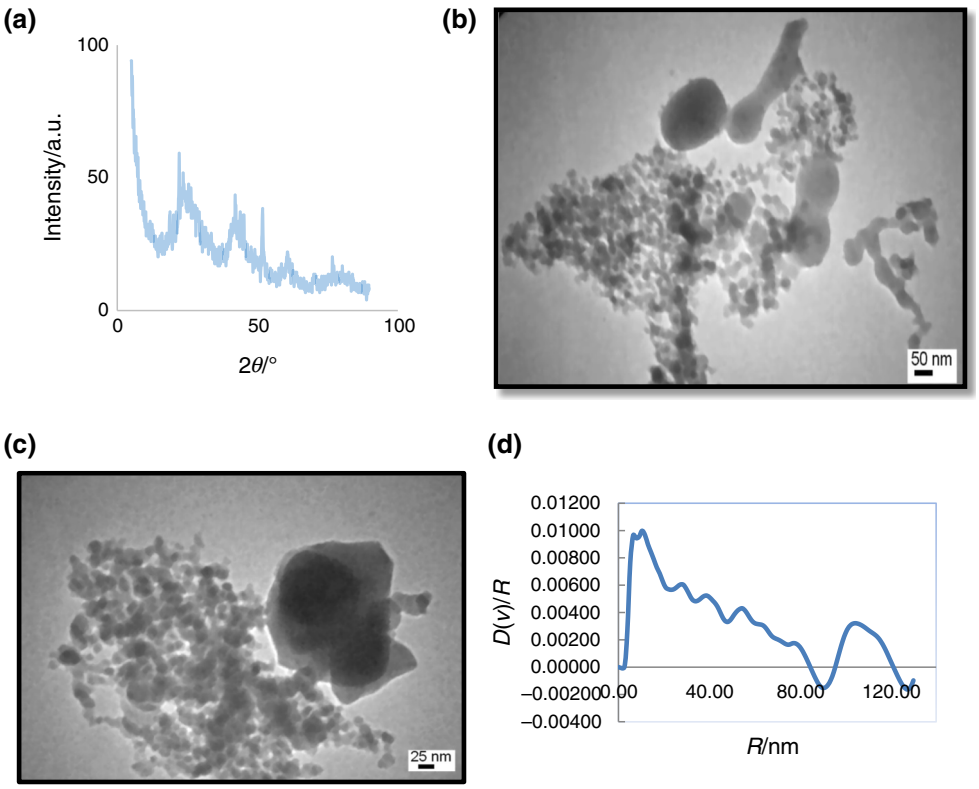

Fig. 3 Characterization of synthesized boron nanoparticles (sample B6), XRD pattern (**a**), TEM images in two different magnifications (**b**, **c**) and SAXS analysis (**d**), respectively

decomposition of AP and formation of an intermediate product. Finally, the last event, namely high-temperature decomposition (HTD) which is also an exothermic process and happens at the temperatures higher than 350 °C (HTD = 402.8 °C), is attributable to the complete decomposition of the intermediate product into volatile product. Overall decomposition reaction of AP particles is as follows [19–23]:

$$\begin{aligned} NH_4ClO_4 &\Leftrightarrow NH_4^+ + ClO_4^- \Leftrightarrow NH_3(g) + HClO_4(g) \\ &\Leftrightarrow NH_3(s) + HClO_4(s) \end{aligned} \quad (1)$$

Also, the two steps of pure AP decomposition were distinguishable in the TG mass curves. For pure AP, the mass loss during low-temperature decomposition (LTD) and high-temperature decomposition (HTD) was 29 and 70%, respectively (Fig. 4a). As shown in Fig. 4a and summarized in Table 2, consecutive and wide temperature range of thermal decomposition of pure AP particle with two mass loss steps could also be deduced from TG curve in which two clear peaks occurred.

Thermal analysis of AP + B nanocomposite

The effects of content and average particle size (APS) of boron micro, nanoparticles- and nanorods on the decomposition characteristics of treated ammonium perchlorate particles, obtained through DSC/TG experiments, are summarized in Table 2 and Fig. 4. The micro- and nanocatalyst contents and average particle size (APS) not only affect the decomposition temperature of ammonium perchlorate particles, but also may cause a significant alteration of decomposition reaction enthalpy.

Figure 4b represents DSC/TG curves of AP + B (μ5) microcomposites. Although the DSC and TG curves are nearly similar with those obtained for pure AP, but the thermal events were found to shift to higher temperatures. The partial thermal decomposition event, with 30% mass loss and maximum temperature of 314 °C, was observed in the range of 274–340 °C. Also, complete decomposition temperature of AP particles with maximum at 412.3 °C was seen in the range of 366–450 °C accompanied by 70% mass loss. As it could be observed from these data, and in contrast with the results obtained for pure AP, extent of mass loses ($\Delta m = 100\%$) and temperature range of decomposition changed upon presence of microboron and heat of decomposition decrease from 580.0 to 458.0 J g^{-1}. This undesirable property may be related to large content of oxide layer, B_2O_3, which prevent appropriate catalytic effects. The summary of DSC/TG experiments results of AP + B (μ2) and AP + B (μ5) microcomposites are presented in Table 2.

Figure 4c, d and Table 2 show the differential thermal analysis (DSC/TG) results of AP + B nanocomposites with different content, size and structure. Based on the

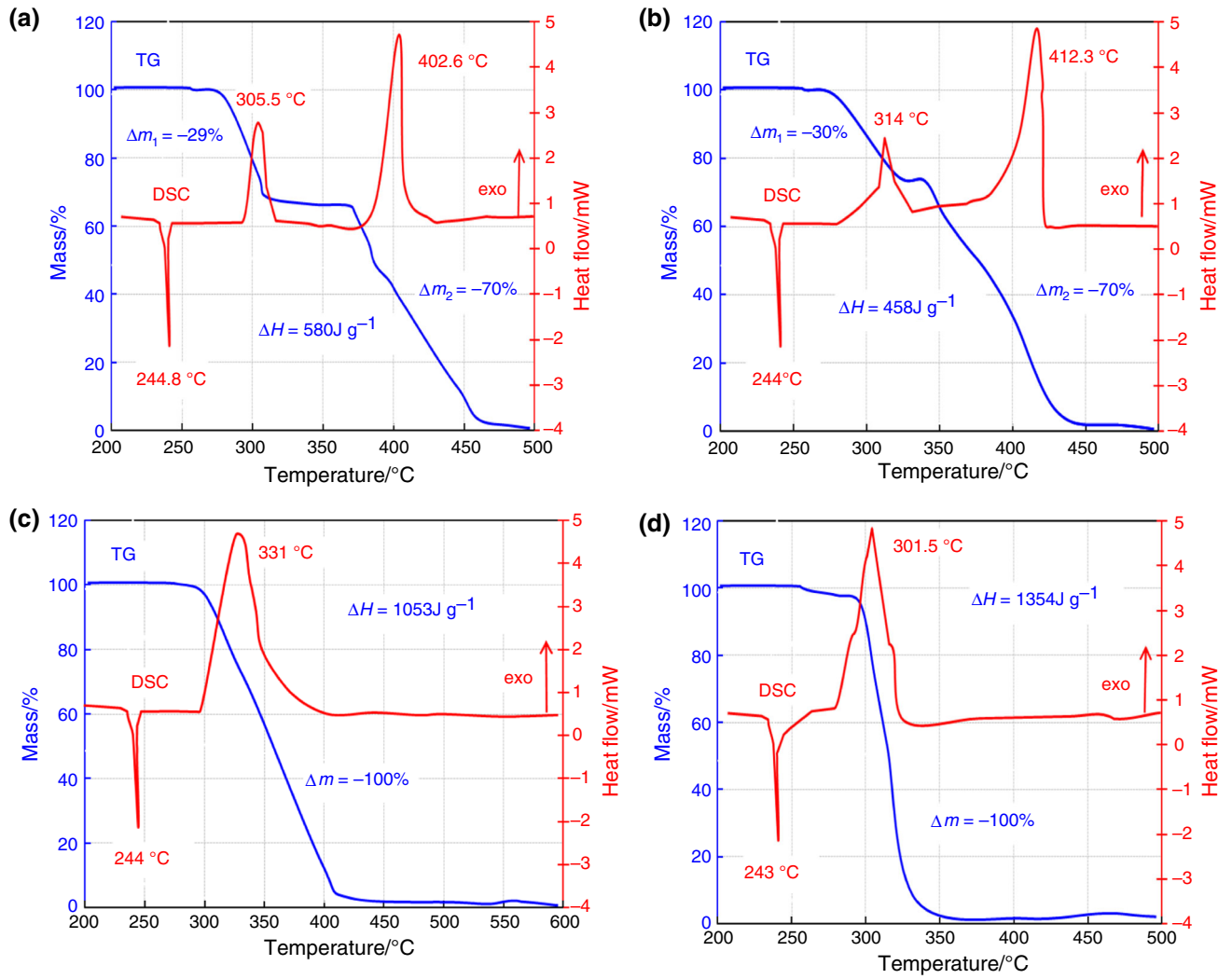

Fig. 4 Thermal analysis of pure AP with mean particle size of 80–100 μm (**a**), and containing 95:5 composites, AP + Bμ, AP + B2 (nanorods) and AP + B6 (nanoparticles) particles (**b**–**d**), respectively

illustrated result in Table 2, all AP + B nanocomposites in the presence of 2 and 5% of B nanostructure (nanoparticles and nanorods) with different average particle size (APS) have considerably lower decomposition temperature and higher decomposition enthalpy with respect to the pure one. However, evaluations of results show that in the presences of each nanostructure, the catalytic effects will be increased by increasing the content of B nanostructure (Table 2). On the other hand, based on the obtained result in Fig. 5, the catalytic effects will be increased by replacing nanorods with nanoparticles from B2 to B6, and high decomposition temperature (HTD) of pure AP particles reduced from 402.6 to 331 and 301.5 °C from AP + 5% B2 to AP + 5% B6 nanocomposites samples, respectively. Also, as shown in Fig. 5 the same trend occurred in heat of decomposition reaction of AP + B nanocomposites.

However, based on the result in Fig. 5 and Table 2, nanoparticles of boron with the smallest average particle size (25–40 nm) and the highest content (AP7) have the most significant catalytic effect including decrease in decomposition temperature of AP + B nanocomposite by 100 °C and increase in the heat of decomposition from 580 to 1354 J g^{-1}.

Kinetic measurements

The solid-state reactions are associated with the kinetic complication due to their multi-phase characteristics. So, some approximate methods are usually being used for determination of kinetic parameters from the thermal data [19]. In this work, two thermal analysis kinetic methods containing Kissinger and Ozawa were jointly exploited to process the DSC and TG data to extract the kinetic

parameters containing the activation energy (E_a) and the pre-exponential factor (A) for the decomposition of the AP + B nanocomposites (AP + B2 and AP + B6) with two nanocatalyst additives. The DSC and TG curves obtained at various heating rates (β) for AP/B nanocomposite (pure AP, AP + B2 and AP + B6) samples are summarized in Table 3. It is clear that by increasing the heating rate, the decomposition temperature of the samples was shifted to higher temperatures. Based on the result of the end column of Table 3, the same trend was observed in heat of decomposition reaction of nanocomposites. These shifts in heat of decomposition and maximum peak temperature (T_m) of all treated AP particles are summarized in Table 3.

Kissinger method

The Kissinger method was used to determine the Arrhenius parameters for the thermal decomposition of all samples [19]. In order to calculate the pre-exponential factor (A), it was assumed that the decomposition reaction follows first-order kinetics.

The plots of the ln ($\beta\ T_m^{-2}$) against $1/T_m$ were straight lines for pure and treated AP particles (Fig. 6), which indicated that thermal decomposition of these samples follows the first-order kinetic law [19]. The slope of the lines was equal to $-E_a/R$. Therefore, the activation energy (E_a) was obtained from the slope of the graph while the logarithm of the pre-exponential factor, log (A), was calculated from the expression given in ASTM E698 [19]:

$$A = \beta E_a \exp[E_a/RT_m]/RT_m^2 \quad (2)$$

Table 4 contains the calculated values of activation energy and pre-exponential factor for pure and treated AP particles by Kissinger method.

Ozawa method

On the other hand, activation energy (E_a) for all samples was calculated by Ozawa method [19]. In this method, activation energy could be determined from plots of the logarithm of the heating rate versus the inverse of the temperature at the maximum reaction rate in constant heating rate experiments. The activation energy can be determined by Ozawa method without a precise knowledge of the reaction mechanism, using the following equation:

$$\log \beta + 0.496(E_a/RT_m) = C \quad (3)$$

As shown in Fig. 6, the plots of logarithm of heating rates versus reciprocal of the absolute peak temperature for the treated samples were straight lines, which indicated that the mechanism of thermal decomposition of samples over this temperature range did not vary [19]. The activation

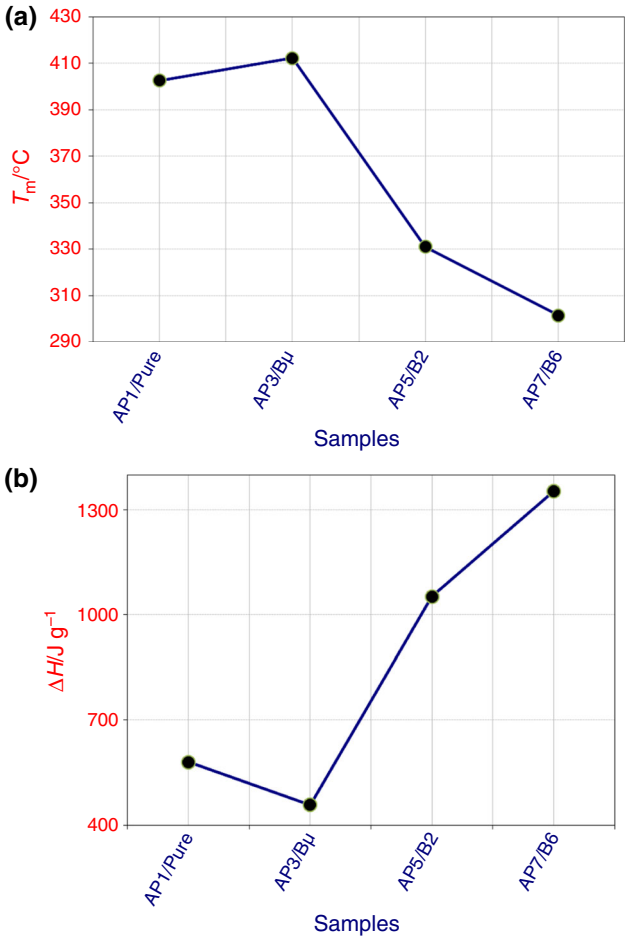

Fig. 5 Effect of particle size of micro- and nanocatalysts on the high-temperature decomposition (HTD) (**a**), and heat of decomposition reaction (ΔH) of AP/B micro- and nanocomposites in the presence of 5 mass% B [pure AP, AP + Bμ, AP + B2 (nanorods) and AP + B6 (nanoparticles)] (**b**)

Table 3 Effect of heating rate on the maximum temperature and the heat of decomposition of AP/B nanocomposites in the presence of 5% of different nanoparticles (B2 and B6), (β = 10 C min^{-1})

Sample no./component	β/°C min^{-1}	Peak T_m/°C	ΔH/J g^{-1}
AP1/(Pure AP)	5	395.3	570
	10	402.6	580
	15	412.0	587.3
	20	419.0	582.3
AP5/(AP + B2)	5	325	1021
	10	331	1053
	15	344.5	1078
	20	354	1098
AP7/(AP + B6)	5	295.0	1325
	10	301.5	1354
	15	316.0	1391
	20	325.0	1398

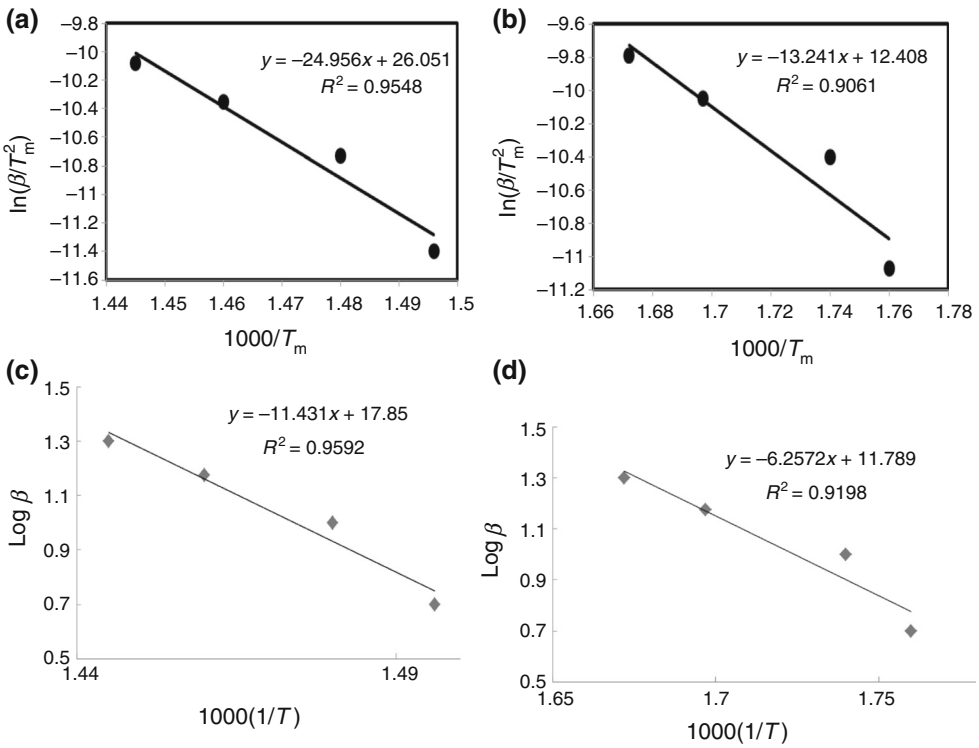

Fig. 6 Plot of ln ($\beta\, T_m^{-2}$) against $1/T_m$ for thermal decomposition of pure AP particles (**a**), AP + 5% B6 nanocomposites particles (**b**) and plot of log β against $1/T_m$ for thermal decomposition of pure AP particles (**c**) and AP + 5% B6 nanocomposites particles (**d**)

Table 4 Comparison of kinetic parameters for decomposition reaction of pure and AP + B nanocomposites sample with different kinetic methods

Method	Kissinger			Ozawa		
Sample no./component	E_a/kJ mol^{-1}	log A/s^{-1}	r	E_a/kJ mol^{-1}	log A/s^{-1}	r
AP1/(Pure AP)	207.5 ± 0.5	15.7 ± 0.2	0.9771	191.6 ± 0.4	14.4 ± 0.2	0.9794
AP5/(AP + B2)	126.4 ± 0.2	10.4 ± 0.4	0.9500	117.9 ± 0.6	9.7 ± 0.5	0.9565
AP7/(AP + B6)	110.1 ± 0.4	9.5 ± 0.5	0.9512	104.9 ± 0.2	9.03 ± 0.06	0.9590

energies were calculated by the Ozawa method summarized in Table 4.

Table 4 shows the calculated kinetic parameters of thermal decomposition of pure and treated AP particles in the presence of boron nanostructures with different particle size (pure AP, AP + B2 and AP + B6 samples) by Kissinger and Ozawa methods.

The results clearly show that in the presence of boron NPs a considerable reduction in the apparent activation energy (E_a) of thermal decomposition of treated AP particles (AP + 5% B6) occurred. Based on the calculated result, in the presence of 5% B6, values of E_a were reduced to 110 kJ mol^{-1}, that is nearly half of pure ones. Also, the same trend occurred for pre-exponential factor, log (A), and decreased considerably in the nanocomposites with respect to pure AP.

Comparison with literature results

The sonochemical method compared with the other methods which have been used for preparing the boron nanostructures [3–6] is very fast, and it does not need high temperatures during the reactions; using the surfactants is not necessary for this method, and the other advantage of using ultrasound radiation is that it yields smaller particles [24]. The effects of ultrasound radiation on chemical reactions are due to the very high temperatures and pressures that develop during the sonochemical cavity collapse by acoustic cavitation. There are two regions of sonochemical activity, as postulated by Suslick et al. [25–27], the inside of the collapsing bubble and the interface between the bubble and the liquid, which extends to about 200 nm from the bubble surface. If the reaction takes place inside the collapsing bubble, as is the case for transition metal carbonyls in organic solvents, the temperature inside the cavitation bubble can be from 4827 to 2027 °C depending on the vapor pressure of the solvent [25]. If water is used as the solvent, the maximum bubble core temperature that can be attained is close to 3727 °C [28]. The product obtained in this case will be amorphous as a result of the high cooling rates (>10^{10} °C s^{-1}) reached

during collapse. On the other hand, if the reaction takes place at the interface, where the temperature has been measured to be 1627 °C [25], one expects to get nanocrystalline products. If the solute is ionic, and hence has a low vapor pressure, then during sonication the amount of the ionic species will be very low inside the bubble and little product is expected to occur inside the bubbles [29]. Since in the present study the solute is non-ionic, and we get amorphous boron particles, we propose that the formation of the boron nanoparticles occurs at the inside of collapsing bubble.

On the other hand, boron is a typical energetic material which produces high heat by oxidation reaction. Thus, fine boron particles expected to have higher catalytic activity on thermal decomposition of AP particles with respect to other traditional nanostructures [18–20]. Although our prepared boron nanostructures present proper catalytic activity, comparing the results of this investigation with other works [18–23] illustrated that our prepared boron nanostructures do not show excellent catalytic activity to improve thermal behavior of AP particles. These properties may be explained that in the first exothermic decomposition step of AP, a solid decomposition reaction occurs to produce large amount of N_2O, O_2, Cl_2, H_2O, HCl and a small amount of NO. Because of higher activity of boron in the presence of produced O_2 in reaction media, a thin layer of B_2O_3 around the nanoparticles and nanorods of boron appears that did not let all nanoboron to affect further the thermal behavior of AP. Produced layer of B_2O_3 in nanorods of boron prevents boron to behave like a perfect catalyst and deactivates boron nanorods much more than nanoparticles of boron. Further study must be done in order for the detailed evaluation of thermal decomposition mechanism of AP particles in the presence of boron nanostructure to get excellent catalytic activity.

Conclusions

Here, we describe a simple method to prepare nanoparticles and nanorods of boron by using ultrasound irradiation. As-prepared microboron by magnesiothermic reduction was used as a precursor to produce nanoboron. Concentrations of boron and sonication time affect size and morphology of final boron particles. By this method, nanoparticles of boron with 30 nm diameter were prepared. Nanoparticles of boron were influenced the exothermic process and gathered both process to one and increase the energy level till 1354 J g^{-1}. Also, nanorods were influenced the energy of AP's decomposition up to 1053 J g^{-1}. In our best knowledge, this is the first report for synthesis of boron nanostructures by using ultrasound irradiation and also the first one on the affect of nanostructured boron on thermal decomposition of ammonium perchlorate particles.

References

1. Spalding MJ, Krier H, Burton RL. Boron suboxides measured during ignition and combustion of boron in shocked Ar/F/O_2 and Ar/N_2/O_2 mixtures. Combust Flame. 2000;120:200–10.
2. Eisenrecih N, Liehmann W. Emission spectroscopy of boron ignition and combustion in the range of 0.2 lm to 5.5 lm. Propellants Explos Pyrotech. 1987;12:88–91.
3. Kuwahara T, Kubota N. Role of boron in burning rate augmentation of AP composite propellants. Propellants Explos Pyrotech. 1989;14:43–6.
4. Slutsky VG, Tsyganov SA, Severin ES, Polenov LA. Synthesis of small-scale boron-rich nano size particles. Propellants Explos Pyrotech. 2005;30:303–9.
5. Pickering L, Mitterbauer C, Browning ND, Kauzlarich SM, Power PP. Room temperature synthesis of surface-functionalised boron nanoparticles. Chem Commun. 2007;6:580–2.
6. Xu TT, Zheng J-G, Wu N, Nicholls AW, Roth JR. Crystalline boron nanoribbons: synthesis and characterisation. Nano Lett. 2004;4:963–8.
7. Suslick KS, Choe S-B, Cichowlas AA, Grinstaff MW. Sonochemical synthesis of amorphous iron. Nature. 1991;353:414–6.
8. Sugimoto M. Amorphous characteristics in spinel ferrites containing glassy oxides. J Magn Magn Mater. 1994;133:460–2.
9. Landau MV, Vradman L, Herskowitz M, Koltypin Y. Ultrasonically controlled deposition–precipitation: Co–Mo HDS catalysts deposited on wide-pore MCM material. J Catal. 2001;201:22–36.
10. Wang H, Lu YN, Zhu JJ, Chen HY. Sonochemical fabrication and characterization of stibnite nanorods. Inorg Chem. 2003;42:6404–11.
11. Zhang JH, Chen Z, Wang ZL, Ming NB. Sonochemical method for the synthesis of antimony sulfide microcrystallites with controllable morphology. J Mater Res. 2003;18:1804–8.
12. Ding T, Zhu JJ, Hong JM. Sonochemical preparation of HgSe nanoparticles by using different reductants. Mater Lett. 2003;57:4445–9.
13. Kadiresh PN, Sridhar BTN. Experimental study on ballistic behaviour of an aluminised AP/HTPB propellant during accelerated aging. J Therm Anal Calorim. 2010;100:331–5.
14. Rocco JAFF, Lima JES, Frutuoso AG, Iha K, Ionashiro M, Matos JR, Suárez-Iha MEV. TG studies of a composite solid rocket propellant based on HTPB-binder. J Therm Anal Calorim. 2004;77:803–13.
15. Rocco JAFF, Lima JES, Frutuoso AG, Iha K, Ionashiro M, Matos JR, Suárez-Iha MEV. Thermal degradation of a composite solid propellant examined by DSC. J Therm Anal Calorim. 2004;75:551–7.
16. Liu L, Li F, Tan L, Li M, Yang Y. Effects of metal and composite nanopowders on the thermal decomposition of ammonium perchlorate (AP) and the ammonium perchlorate/hydroxyterminated polybutadiene (AP/HTPB) composite solid propellant. Chin J Chem Eng. 2004;12:595–8.
17. Duan H, Lin X, Liu G, Xu L, Li F. Synthesis of Co nanoparticles and their catalytic effect on the decomposition of ammonium perchlorate. Chin J Chem Eng. 2008;16:325–8.
18. Hobbs DZ, Campbell TT, Block FE. Methods used in preparing boron. Washington, DC: U.S. Dept. of the Interior, Bureau of Mines; 1964.
19. Eslami A, Hosseini SG, Bazrgary M. Improvement of thermal decomposition properties of ammonium perchlorate particles using some polymer coating agents. J Therm Anal Calorim. 2013;113:721–30.
20. Eslami A, Hosseini SG. Improving safety performance of lactose-fueled binary pyrotechnic systems of smoke dyes. J Therm Anal Calorim. 2013;104:671–8.

21. Hosseini SG, Alavi MA, Ghavi A, Hosseini SJ, Agend F. Modeling of burning rate equation of ammonium perchlorate particles over Cu–Cr–O nanocomposites. J Therm Anal Calorim. 2015;119:99–109.
22. Hosseini SG, Abazari R, Gavi A. Pure $CuCr_2O_4$ nanoparticles: synthesis, characterization and their morphological and size effects on the catalytic thermal decomposition of ammonium perchlorate. Solid State Sci. 2014;37:72–9.
23. Hosseini SG, Ahmadi R, Ghavi A, Kashi A. Synthesis and characterization of α-Fe_2O_3 mesoporous using SBA-15 silica as template and investigation of its catalytic activity for thermal decomposition of ammonium perchlorate particles. Powder Technol. 2015;278:316–22.
24. Aharon G. Using sonochemistry for the fabrication of nanomaterials. Ultrason Sonochem. 2004;11:47–55.
25. McNamara WB, Didenko YT, Suslick KS. Sonoluminescence temperatures during multi-bubble cavitation. Nature. 1999;401:772–5.
26. Suslick KS, Hammerton DA, Cline RE. Sonochemical hot spot. J Am Chem Soc. 1986;108:5641–2.
27. Grinstaff MW, Cichowlas AA, Choe SB, Suslick KS. Effect of cavitation conditions on amorphous metal synthesis. Ultrasonics. 1992;30:168–72.
28. Misik V, Miyoshi N, Riesz P. EPR spin-trapping study of the sonolysis of H_2O/D_2O mixtures: probing the temperatures of cavitation regions. J Phys Chem. 1995;99:3605–11.
29. Jeevanandam P, Koltypin Y, Palchik O, Gedanken A. Synthesis of morphologically controlled lanthanum carbonate particles using ultrasound irradiation. J Mater Chem. 2001;11:869–73.